EQUILIBRIUM JOURNAL OF CHEMICAL ENGINEERING
*Homepage:*https://jurnal.uns.ac.id/equilibrium

Calcination Temperature Effect on Characteristic Properties of $Na_{2/3}[Fe_{1/2}Mn_{1/2}]O_2$ Synthesized by Sol-Gel Reaction

Diah Agustina Puspitasari[a*], Supriyono[a], Christina Wahyu Kartikowati[a], Mar'atul Fauziyah [a], Femiana Gapsari [b], Vania Mitha Pratiwi [c], Devina Annora H Br Butar-Butar[a], Ira Marisa D.N[a], Rashieka Putri Maghfiroh[a], Yudha Bhakti Prasetia[a], Rivanda Adi I. R [a], Irginata Aqil H [a], Roihan Rajabi[a], Umar Khalid Zaki Abdul[a]

[a] *Departement* of *Chemical Engineering, Faculty of Engineering, Universitas Brawijaya, Malang, Indonesia 65145*
[b] *Department of Mechanical Engineering, Faculty of Engineering, Universitas Brawijaya, Malang, Indonesia 65145*
[c]*Department of Material and Metallurgical, Faculty of Industrial Technology and Systems Engineering, Institut Teknologi Sepuluh Nopember, Surabaya, Indonesia*

[*]Corresponding author: deeaja_chemeng@ub.ac.id

DOI: *https://dx.doi.org/10.20961/equilibrium.v8i1.80464*

Article History
Received: 16-11-2023, Accepted: 30-04-2024, Published: 02-05-2024

Keywords: Sol-Gel, Solid State, Grain Growth, Calcination, $Na_{2/3}[Fe_{1/2}Mn_{1/2}]O_2$

ABSTRACT. Recently, $Na_{2/3}[Fe_{1/2}Mn_{1/2}]O_2$ has received attention as a potential candidate material for cathode sodium-ion batteries. However, this material was synthesized by a solid-state process, resulting in larger particle size and nonuniform morphology. The larger particle size will sluggish the Na ion diffusion. Here we report the synthesis of $Na_{2/3}[Fe_{1/2}Mn_{1/2}]O_2$ using a simple sol-gel process. The X-ray diffraction revealed that the sample was identified as $Na_{2/3}[Fe_{1/2}Mn_{1/2}]O_2$ with a hexagonal crystal structure. However, the impurities are formed at diffraction angles of 36.28°, 45.03°, and 51.23°. Calcination temperature affects the formation of the crystal phase, grain growth, morphology, and particle size. Our findings provide valuable insight into the development of $Na_{2/3}[Fe_{1/2}Mn_{1/2}]O_2$ material with desirable properties.

1. INTRODUCTION

Sodium-ion batteries (SIB) have received attention recently due to their abundant sources, non-toxicity, and affordable prices. The most considerable sodium content on earth comes from seawater (2.6%) [1-3]. SIB has a working principle like lithium-ion battery (LIB), providing an excellent opportunity to be applied as a battery. However, the application of SIB for EVs faces challenges; the ionic radii of the Na^+ ion (1.02 Å) are larger than the Li^+ ion (0.76 Å), resulting in low diffusion of Na^+ ions from/into the active material during the charging/discharging process, thereby decreasing the energy density and hinder practical application [4-6]. Developing high-performance electrode materials is the key issue for developing practical SIB.

Various Na-containing compounds have been intensively studied as cathode materials for SIBs. Among them, layered sodium transition metal oxides $NaxMO_2$ (M= Mn, Co, Cr, Fe, and V) with different structures are the most important class of cathode materials [7, 8] because they can deliver a high capacity. The P2-$Na_{2/3}Fe_{1/3}Mn_{2/3}O_2$ cathode materials are fascinating due to their large discharge capacity and high energy density. The P2-$Na_{2/3}Fe_{1/3}Mn_{2/3}O_2$ is made from an earth-abundant material with a theoretical capacity of 190 mAh/g [9, 10]. Up to now, the $Na_{2/3}[Fe_{1/2}Mn_{1/2}]O_2$ composite materials were synthesized by solid-state. However, most of the reports showed that the morphology is irregular and control of uniform particle size distribution has not yet been achieved, which affected the electrochemical performance. Komaba., et al.[11] reported that the P2-$Li_{2/3}Ni_{1/3}Mn_{2/3}O_2$ showed a particle size up to 3 μm using the solid-state ion exchange method. Saxena et al. [12] reported that the particle size of P2-$Na_{2/3}Fe_{1/3}Mn_{2/3}O_2$ increased to 1.3 μm at 950 ºC. The larger particle size will trigger sluggish sodium ion diffusion, resulting in the fading of discharge capacity.

In this work, the P2-$Na_{2/3}Fe_{1/3}Mn_{2/3}O_2$ was first synthesized using a simple sol-gel process by controlled heat treatment process as prospective material, which will act as a cathode for sodium-ion battery. The sol-gel technique intends to desirably control the dimensions of a material on a nanometer scale from the initial stages of processing. Chemical processing controlled high purity and better homogeneity can be used to enhance the properties of materials. This lower-temperature processing technique is a major advantage over the conventional methods of nanoparticle synthesis [13, 14].

The crystal phases and morphology properties of $Na_{2/3}Fe_{1/3}Mn_{2/3}O_2$ samples are systematically studied, and their correlation is discussed in detail. The crystal structure of P2-$Na_{2/3}Fe_{1/3}Mn_{2/3}O_2$ has been formed, and its particle size is smaller than that of the previous report.

2. MATERIALS AND METHODS

2.1 Material synthesis of $Na_{2/3}[Fe_{1/2}Mn_{1/2}]O_2$ (NFMO)

The $Na_{2/3}[Fe_{1/2}Mn_{1/2}]O_2$ (NFMO) samples were prepared by a sol-gel method using Fe_2O_3, Mn_2O_3, and Na_2CO_3 were dissolved in 40 ml of demineralized water (DI) with stirring for 6 hours. Then, the precursor solution was evaporated until a green gel was formed. The gel was then dried at 120 °C for 12 hours, continuing with the calcination. The dry gel was pre-heated at 450 °C for 4 hours and followed with the calcination at 650-750 °C for 8 hours in air atmospheric. The NFMO material calcined at various temperatures were called NFMO-650, NFMO-700, and NFMO-750.

2.2 Material charactirization of $Na_{2/3}[Fe_{1/2}Mn_{1/2}]O_2$

The $Na_{2/3}[Fe_{1/2}Mn_{1/2}]O_2$ material was characterized with X-ray diffraction (XRD) analysis (Bruker D8 ADVANCE) with Cu Kα radiation parameters (λ = 1.5418 Å). Scanning electron microscopy (SEM-EDS) (SEM; SU8220). The crystal size was calculated using the Scherrer method based on the full width at half-maximum of the diffraction peaks (FWHM).

3. RESULTS AND DISCUSSION

The X-ray diffraction (XRD) pattern of samples NFMO-650, NFMO-700, and NFMO-750 are shown in Figure 1. The XRD pattern revealed that all samples indicates P2 phases with space group P63/mmc which is complement very well with the diffraction standart COD number 96-400-2261. As the calcination temperature increases, the peak width of NFMO becomes narrower, and the relative intensity of the characteristic peaks gradually increases, indicating that the crystal structure of NFMO is formed. Phase formation is related to grain growth which is caused by surface and bulk diffusion . It is well known that the phase formation during the grain growth is controlled by the mobility of the atoms. Moreover the phase formation is affected by synthesis parameters as substrate temperature and degree of ionization [15] . The crystal size was calculated using the Scherrer equation as seen in equation 1 [16].

$$D = \frac{k\lambda}{\beta \cos\theta} \qquad (1)$$

Where D is the average crystallite size, k is Scherer's constant (0.96), λ is X-ray wave length (1.5406 Å), and β is full witdh at half maxima at diffraction angle 2θ.

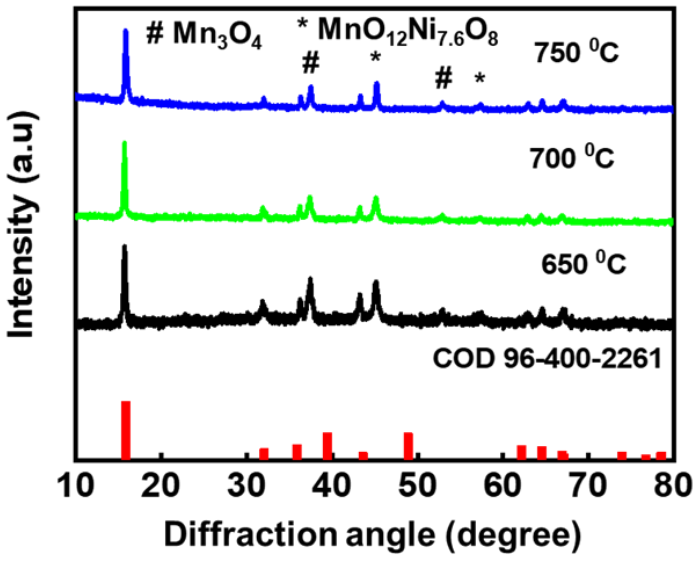

Figure 1. Diffraction pattern of NFMO at various temperature

The average crystal sizes are 15.55 nm, 21.78 nm, and 63.98 nm for samples NFMO-650, NFMO-700, and NFMO-750, respectively. The higher temperature will enhanced the ion diffusion which triggering the crystal growth rate result in increasing the crystal size. Furthermore, the heat treatment temperature improved the progressing of diffraction peak growth and intensity with formation of a better crystallinity [17, 18]. However, the impurities appear at the diffraction angles of 36.28°, 45.03°, 51.23°, and 57.29° and have different intensity levels related to $Mn_{0.2}Ni_{7.6}O_8$ and Mn_3O_4 compounds. This ascribe that MnO dosen't cooperate well in NFMO matrix at temperature range 650-750 °C. It might need the higher calcination temperature and further investigate.

The morphology of NFMO were investigated in detail by using SEM, as shown Figure 2a-b. The SEM images revealed similiar characteristic for NFMO-650 and NFMO-750 materials, exhibiting irregular morphology and agregation. The NFMO-650 exhibits some aggregation and the particle size up to 143 nm. However the NFMO-750 revealed increasing the agregation degree with the particle size 196 nm as seen in Figure 2b. The increasing calcination temperature will enlarge the grain boundaries, increasing the particle size. The smaller particles have a higher surface energy than that in the bulk. Therefore, the increasing calcination temperature will trigger a decrease in surface energy. As a result, the small particles will combine to form larger particles [15, 19, 20]. These result in line with the X-ray diffraction analysis. However, although the particle size increases, smaller particle dispersion can still be observed at higher calcination temperatures.

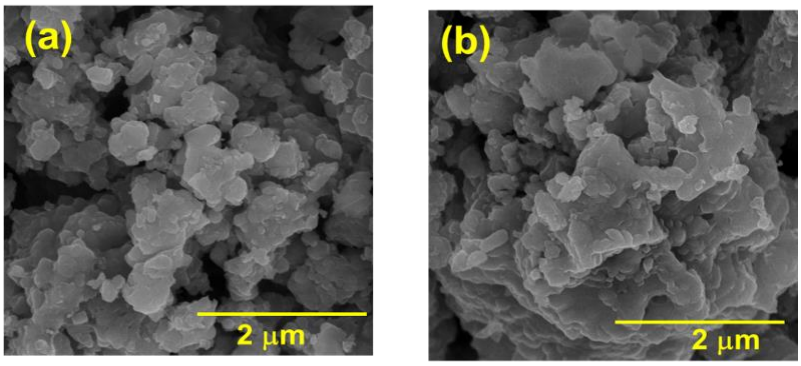

Figure 2. SEM analysis at various temperatures: (a) NFMO-650 dan (b) NFMO-750

4. CONCLUSION

NFMO composite material was successfully synthesized using the sol-gel method. The calcination temperature affects the characteristics of the NFMO cathode material, which can be seen in the formation of a crystal phase at a higher temperature, accompanied by a larger crystal size. Based on morphological analysis, it can be seen that temperature affects morphology and particle size. Our works provides valuable insight and guidelines for developing layer oxide material for sodium ion battery application.

ACKNOWLEDGEMENTS

We want to thank the Faculty of Engineering, Brawijaya University, for funding and supporting the research grant of Hibah Doktor Non-Lektor Kepala with contract number 70/UNI0/PN2023.

REFERENCES

1. Ni, Q., Bai, Y., Wu, F., and Wu, C. Polyanion-Type Electrode Materials for Sodium-Ion Batteries. *Adv Sci*, **2017**. 4(3): p. 1-24.
2. Khan, S.A., Ali, S., Saeed, K., Usman, M., and Khan, I. Advanced cathode materials and efficient electrolytes for rechargeable batteries: practical challenges and future perspectives. *Journal of Materials Chemistry A*, **2019**. 7(17): p. 10159-10173.
3. Hirsh, H.S., Li, Y., Tan, D. H. S., Zhang, M., Zhao, E., and Meng, Y. S. Sodium-Ion Batteries Paving the Way for Grid Energy Storage. *Advanced Energy Materials*, **2020**. 10(32): p. 1-8.
4. Wu, F., Zhao, C., Chen, S., Lu, Y., Hou, Y., Hu, Y. -S., Maier, J., and Yu, Y. Multi-electron reaction materials for sodium-based batteries. *Materials Today*, **2018**. 21(9): p. 960-973.
5. Zhu, Y., Xua, H., Maa, J., Chena, P., and Chen, Y. The recent advances of NASICON-$Na_3V_2(PO_4)_3$ cathode materials for sodium-ion batteries. *Journal of Solid State Chemistry*, **2023**. 317: p. 123669.
6. Zhao, L.N., Zhang, T., Zhao, H. L, and Hou, Y. L. Polyanion-type electrode materials for advanced sodium-ion batteries. *Materials Today Nano*, **2020**. 10: p. 1-26.

7. Buchholz, D., Chagas, L. G., Winter, M., and Passerini, S. *P*2-type layered $Na_{0.45}Ni_{0.22}Co_{0.11}Mn_{0.66}O_2$ as intercalation host material for lithium and sodium batteries. *Electrochimica Acta*, **2013**. 110: p. 208-213.
8. Santamaría, C., Morales, E., Rio, C. d., Herrad´ on, B., Amarillaa, J. M. Studies on sodium-ion batteries: Searching for the proper combination of the cathode material, the electrolyte and the working voltage. The role of magnesium substitution in layered manganese-rich oxides, and pyrrolidinium ionic liquid. *Electrochimica Acta*, **2023**. 439: p. 141654.
9. Zarrabeitia, M., Nobili, F., Lakuntz, O., Carrasco, J., Rojo, T., Cabanas, M. C., and Márquez, M. G. A. M. Role of the voltage window on the capacity retention of P2-$Na_{2/3}[Fe_{1/2}Mn_{1/2}]O_2$ cathode material for rechargeable sodium-ion batteries. *Communications Chemistry*, **2022**. 5(1): p. 1-11.
10. Durmus, Y.E., Zhang, H., Baakes, F., Desmaizieres, G., Hayun, G., Yang, L., Kolek, M., Küpers, V., Janek, J., Mandler, D., Passerini, S., and Ein-Eli, Y. Side by Side Battery Technologies with Lithium-Ion Based Batteries. *Advanced Energy Materials*, **2020**. 10(24): p. 1-21.
11. Komaba, S., Yoshii, K., Ogata, A., and Nakai, I. Structural and electrochemical behaviors of metastable $Li_{2/3}[Ni_{1/3}Mn_{2/3}]O_2$ modified by metal element substitution. *Electrochimica Acta*, **2009**. 54(8): p. 2353-2359.
12. Saxena, S., Vasavana, H. N., Badolea, M., Dasa, A. K., Deswalb, S., Kumarb, P., and Kumar, S. Tailored P2/O3 phase-dependent electrochemical behavior of Mn-based cathode for sodium-ion batteries. *Journal of Energy Storage*, *2023*. 64: p. 107242.
13. kumar, A., Yadav, N., Bhatt, M., Mishra, N. K., Chaudhary, P., and Singh, R. Sol-Gel derived nanomaterials and it's Applications: A Review. *Research journal of chemical science*, **2015** (912)*:p. 1-6.*
14. Yarbrough, R., Davis, K., Dawood, S., and Rathnayake, H. A sol-gel synthesis to prepare size and shape-controlled mesoporous nanostructures of binary (II-VI) metal oxides. *RSC Adv*, **2020**. **10**(24): p. 14134-14146.
15. Marshal, A., Singh, P., Music, D., Wolff-Goodrich, S., Evertz, S., Schkell, A., Johnson, D. D., Dehm, G., Liebscher, C. H., Schneider, J. M. Effect of synthesis temperature on the phase formation of NiTiAlFeCr compositionally complex alloy thin films. *Journal of Alloys and Compounds*, **2021** (854): p. 155178.
16. Muniz, F.T., Miranda, M. A. R., Santos, C. M., and Sasaki, J. M. The Scherrer equation and the dynamical theory of X-ray diffraction. Acta Crystallogr A Found Adv, **2016** (72): p. 385-90.
17. Zaid, M.H.M., Matoria, K. A., Aziza, S. H. A., Kamaria, H. M., Fena, Y. W., Yaakoba, Y., Sa'ata, N. K., Gürolc, A., Şakarc, E. Effect of heat treatment temperature to the crystal growth and optical performance of Mn_3O_4 doped α-Zn_2SiO_4 based glass-ceramics. *Results in Physics*, **2019**. **15**: p. 102569.
18. Babu, C. B., Rao, B. V., Ravia, M., and Babu, S. Structural, microstructural, optical, and dielectric properties of Mn^{2+}: Willemite Zn_2SiO_4 nanocomposites obtained by a sol-gel method. *Journal of Molecular Structure*, **2017**. 1127: p. 6-14.
19. Kusuma, M., and Chandrappa, G. T. Effect of calcination temperature on characteristic properties of $CaMoO_4$ nanoparticles. *Journal of Science: Advanced Materials and Devices*, **2019**. **4**(1): p. 150-157.
20. Singh, R.C., Singh, M. P., Singha, O., and Chandic, P. S. Influence of synthesis and calcination temperatures on particle size and ethanol sensing behaviour of chemically synthesized SnO_2 nanostructures. Sensors and Actuators B: Chemical, 2009. **143**(1): p. 226-232.